Proc. NIPR Symp. Polar Biol., 7, 270–282, 1994

VEGETATION CHANGE DETECTION USING LANDSAT DATA IN NORTHERN FINLAND —A TEST CASE USING SMOOTHING AND LAPLACIAN FILTERING—

Yoshio AWAYA[1], Tuomas HÄME[2] and Nobuhiko TANAKA[1]

[1]*Forestry and Forest Products Research Institute, Tsukuba 305*
[2]*Technical Research Center of Finland, SF-02150 Espoo, Finland*

Abstract: It has been predicted that some boreal tree species would migrate north several hundred meters annually in response to the predicted global warming due to doubling of CO_2 by the middle of the next century. It has also been said that large parts of the boreal forest and tundra would migrate and disappear because of global warming. The average global temperature has already shown a tendency to increase over the past two decades. In the meantime, twenty years have passed since the launching of Landsat 1 and satellite data have been taken since then. The data make it possible to monitor vegetation over a long time. This paper describes the basic concepts to monitor vegetation shifts using satellite data and a system of detection. The system, consisting of a linear-weighting running-average smoothing and a Laplacian filter, was tested using Landsat Multispectral Scanner data for northern Finland. Vegetation boundaries were defined as zero isopleths of the second derivative of a Laplacian-filtered normalized difference vegetation index image. A comparison of boundary lines derived from 1972 and 1987 Landsat data showed small changes in the vegetation boundary, but no clear evidence of vegetation shifts was found.

1. Introduction

It has been pointed out that global climatic change will cause drastic changes in vegetation, especially in the high latitudes. Simulations using various general circulation models have predicted that the global mean annual temperature will increase by 1.5 to 4.5°C by between 2030 and 2050. Temperature increase in winter in the high latitudes may cause the greatest change on the earth, and the growing season will become longer (BOER *et al.*, 1990; SINGH and WHEATON, 1991). A temperature change of 3°C would be equivalent to a 250 km shift in latitude or a 500 m shift in elevation (GATES, 1990). In other words, boreal species would have to be migrating north about 6 km annually to keep up with the shift in their ideal habitat. Also, these temperature increases would accelerate vegetation growth. According to those simulations, global vegetation will suffer from global warming especially in the high latitudes (boreal forests and tundra) and the arid zones (BOER *et al.*, 1990; EMANUEL *et al.*, 1985; GATES, 1990; SINGH and WHEATON, 1991).

Various effects on boreal and tundra vegetation brought on by global

warming have been predicted. A review of these and possibilities of their detection using satellite data are described below.

A pollen study has revealed that boreal coniferous species seemed to have migrated a few hundred meters annually following the glacial retreat in North America (OVERPECK *et al.*, 1991), and potential migrations under CO_2 doubling scenarios have been estimated to be, at most, several hundred meters a year (GATES, 1990; SINGH and WHEATON 1991). The Intergovernmental Panel on Climate Change has reported that some parts of global vegetation could migrate at 10 to 100 meters annually (OHMURA *et al.*, 1991). Since the global temperature would increase too quickly based on these CO_2 doubling scenarios, large parts of the boreal forests will be replaced by cold temperate forests and disappear (EMANUEL *et al.*, 1985). Present land observation satellites are equiped with high resolution sensors (*ex* High Resolution Visible of SPOT has a 20 m ground resolution, Thematic Mapper of Landsat has a 30 m ground resolution.), and these resolution are fine enough to monitor possible vegetation shifts.

Warmer and drier summers will cause more frequent forest fires, forest decline and permafrost melt (SHUGART *et al.*, 1992) which might produce bogs (BORE *et al.*, 1990). Forest fires could be monitored by large area coverage satellite sensors like NOAA Advanced Very High Resolution Radiometer (AVHRR). Since NOAA satellites provide daily coverage of the globe, it is possible to detect forest fires in almost real time. Above all, the 1.1 km ground resolution ability makes it possible to detect major forest fires. However, a lot of effort is necessary to know the tendency for fire occurrence over a large area.

Forest decline has been a major problem in large parts of Europe and North America, and it would occur in large areas because of global warming. Present satellite data have proven poor in detecting early stages of coniferous forest declines, if only single date imagery is used (KENNEWEG *et al.*, 1988). However, good results have been achieved in pine fungi damage detection when change detection techniques using more than one image have been used (HÄME, 1991).

Permafrost thawing yields bogs in the boreal forest. However, forest logging, not an outcome of global warming but a direct human impact, also causes bog formation. Bogs caused by logging are clearly visible in land observation satellite data in Siberia. On the other hand, since natural paludification/depaludification cycle is about 200 to 300 years and their boundary proceeds only a few meters a year (SHUGART *et al.*, 1992), it is impossible using satellite data to detect decadal changes on bog formation caused by global climate changes.

A milder climate would accelerate forest growth (BORE *et al.*, 1990), but a higher CO_2 concentration might suppress tree growth (MOONEY *et al.*, 1991). In either case, it would not be possible to identify such effects on tree growth using satellite data.

A shift in the vegetation boundary would be the easiest to detect using satellite data. Therefore methods of monitoring the boundary shifts were developed and tested using Landsat Multispectral Scanner (MSS) data of which ground resolution was about 80 meters. A study site was selected in an ecotone between the boreal forest and Arctic tundra in northern Finland. The basic

concepts, methods, problems and the possibility of monitoring vegetation changes caused by global warming are reported in this paper.

2. Study Site and Data

A part of the study site (Kevo, around 69°30′N 27°00′E) is in a nature conservation area making it ideal for vegetation monitoring since it is free from any direct human disturbance. The study site extends over to forest-tundra and shrub-tundra zones. A 13°C isotherm of mean July temperature, which represents the northern limit of present boreal forests (SINGH and WHEATON, 1991), runs through the middle of the study site. The main vegetation there is shrub-tundra, dwarf birch (*Betula* spp.) forests and birch-pine (*Pinus sylvestris*) forests. Some portion of the birch forests are subjected to moth (*Epirrita autumnata*) caterpillar damage every now and again. The topography is gentle with numerous lakes. Bedrock is exposed at the top of hills (NATIONAL BOARD of SURVEY, 1988). The annual mean temperature in Finland does not seem to have changed significantly in the last three decades (HEINO, 1992).

Two Landsat MSS images taken on September 1, 1972 and July 18, 1987 (Fig. 2) were used in this study. Both images, which cover 40 km (east to west) by 40 km (north to south), were stored in a hard disk of a Sun Sparc II computer, then the 1972 image was overlaid on the 1987 image and processed using an image processing system called 'ERDAS'.

3. Basic Concepts of Vegetation Monitoring

The following were assumed for changes in vegetation cover due to global warming:

a) Vegetation boundaries will shift in response to global warming.

b) In northern Finland, temperature is the most significant growth factor.

c) Boreal pioneer species would invade the shrub tundra first.

Thus, boundary shifts should be particularly apparent between the boreal forest and shrub tundra.

The changes in the vegetation cover are assumed to cause the following spectral changes:

d) Spectral reflectance in the near infrared region will increase when the biomass increases in sparsely vegetated areas.

e) Since the normalized vegetation index (NDVI,(CH4(MSS)−CH2(MSS))/(CH4(MSS)+CH2(MSS))) is sensitive to the biomass when the leaf area index (LAI) is less than 3 (ASRAR *et al.*, 1989), it should be a good measure of change in vegetated areas.

f) The invasion in the transition zone by boreal pioneer species, especially by birches, should increase the standing biomass and thus the values of the NDVI.

A schematic figure of the expected changes is shown in Fig. 1.

The long term shift of the vegetation boundary would indicate changing climate, whereas a short term—two or three decades—local shift may not

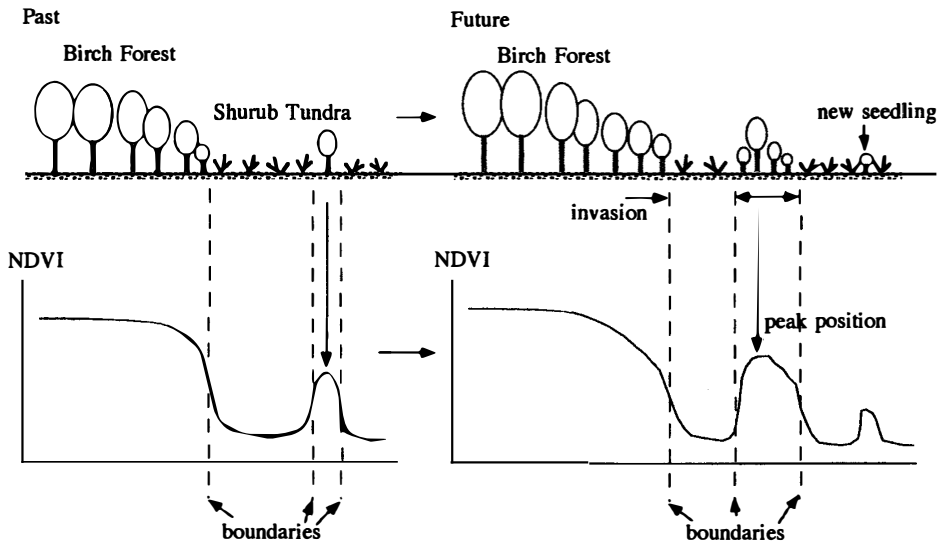

Fig. 1. Schematic Figure of Vegetation Shift in Boreal Forest-Tundra Transition Zone. Boreal pioneer species, ex *birch, grow adjacent to shrub tundra (left). The pioneer species will invade shrub tundra in response to global warming in the future, then vegetation boundaries would move (right).*

necessarily indicate climatic change but only changes in the weather pattern. In other words, effects of climatic change will not appear so soon in the vegetation pattern but should require several decades (SHUGART *et al.*, 1992). Thus, if the boundaries were monitored on a global scale for the long term, magnitudes and geographical patterns of the shifts will show the effects of climatic changes on vegetation.

4. Method

At first, intensities of the 1972 MSS signals were adjusted to those of the 1987 MSS signals using the average digital numbers (DN) from a dark water area (DN 11.9 (CH2), 1.3 (CH4) for 1972, 16.8 (CH2), 10.0 (CH4) for 1987) and bright rock outcrop (DN 40.6 (CH2), 32.7 (CH4) for 1972, 48.0 (CH2), 48.0 (CH4) for 1987) as standard, since they are common to both images and are supposed to be spectrally invariant. Then the NDVI of the two MSS images (Figs. 2, 3) were computed from the radiance values as follows.
Matching intensities:

$$DN72'(i,\ CHj)=(DN72(i,\ CHj)-Water72\ (CHj)) \times\frac{(Rock87\ (CHj)-Water87\ (CHj))}{(Rock72\ (CHj)-Water72\ (CHj))}+Water87\ (CHj). \quad (1)$$

Computing radiance:

$$Rad(i,\ CHj)=(DN(i,CHj)-Water\ 87(i,CHj))\times Gain\ 87\ (CHj). \quad (2)$$

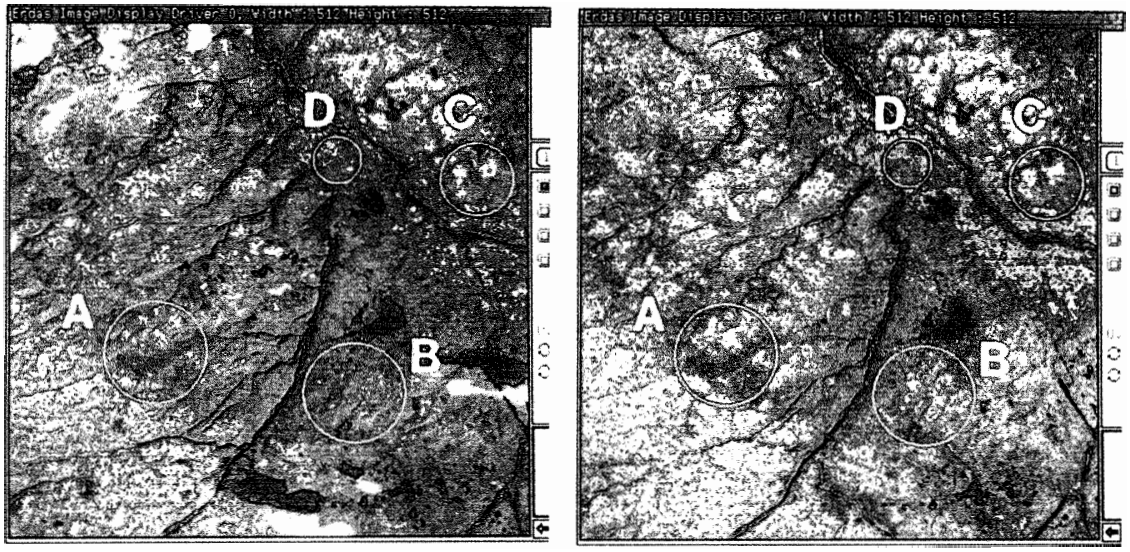

Fig. 2. Landsat MSS Data Over The Test Site (September 1, 1972 (left) and July 18, 1987 (right)). Reddish parts show dense vegetation and blueish parts show rocky areas. Colour changes mainly due to coverage of vegetation and rock within a pixel. Thick and thin clouds covered some parts. The circled areas are cloud free and consist of A:birch mire, birch forest and treeless tundra. B:birch forest and treeless tundra. C:pine forest, birch forest and treeless tundra. D:pine and birch forest.

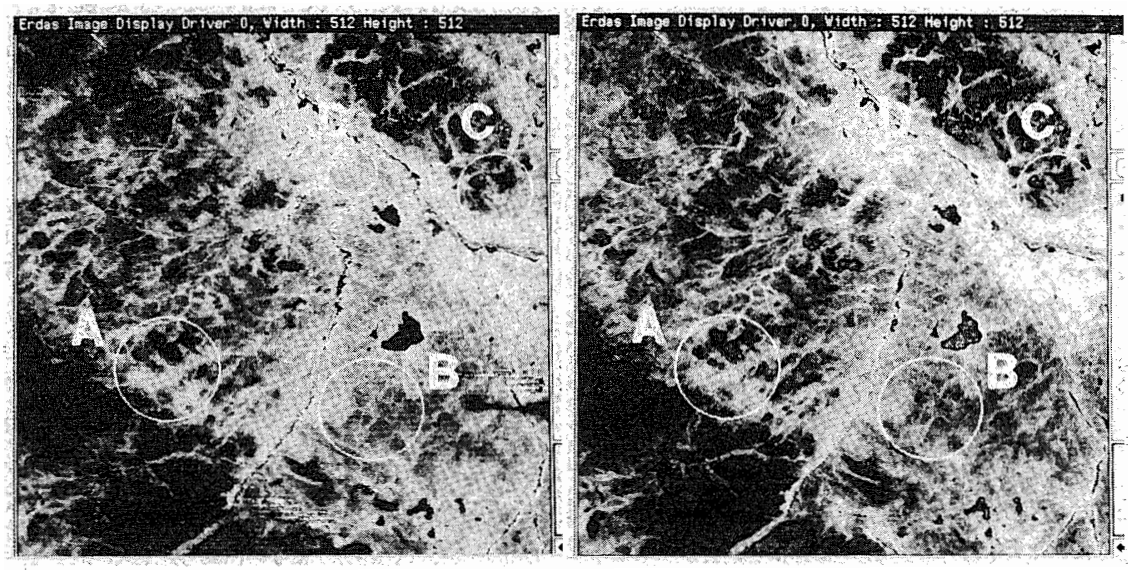

Fig. 3. Normalized Difference Vegetation Index of The 1972 (left) and 1987 (right) Landsat Data. Brighter parts are dense vegetation (ex pine and birch forests). Very dark areas are rocky areas, clouds and water.

Computing NDVI:

$$\mathrm{NDVI}(i)=(\mathrm{Rad}(i,\mathrm{CH4})-\mathrm{Rad}(i,\mathrm{CH2}))/(\mathrm{Rad}(i,\mathrm{CH4})+\mathrm{Rad}(i,\mathrm{CH2})), \quad (3)$$

where

DN72(i,CHj)	is the registered intensity for pixel i in channel j by the MSS sensor in the 1972 data,
DN'72(i,CHj)	computed 1972 MSS DN adjusted to the 1987 MSS DN,
DN(i,CHj)	DN72'(i,CHj) and DN87(i,CHj),
Water72(CHj),Water87(CHj)	the mean intensity of dark water,
Rock72(CHj),Rock87(CHj)	the mean intensity of bright rock,
Rad(i,CHj)	computed radiance (mW/cm^2/sr/μm) (RESTEC, 1986),
Gain87(CHj)	gain of Landsat 5 MSS: 0.0660/DN(CH2), 0.0615/DN(CH4).

Gains of Landsat 5 MSS (RESTEC, 1986) were converted for an 8 bit dynamic range and its unit was also changed from per channel to per micron in the above calculation after dividing by the spectral range of each channel. Reflectance factors of clear water are about 1 to 2 percent around 650 nm (CH2) and almost 0 percent if longer than 700 nm (CH4). Then dark water pixels are often considered showing atmospheric path radiance of a scene, and subtraction of its digital number from pixels of images like that in equation 2 is the most simple and common atmospheric correction.

Profiles were drawn using intensities along several straight lines of three different directions in the two NDVI images (Fig. 4). Though intensities of the NDVI ranges between −1 and 1, they were scaled from 0 to 255 in Figs. 4 and 5. Then differences of edges and peaks between the two NDVI data were examined. The profiles were smoothed as follows using a linear-weighting running-average smoothing (Fig. 5, AWAYA *et al.*, 1992) with 11 pixels to remove noise and to know major patterns of the NDVI profiles.

Smoothing of NDVI profiles:

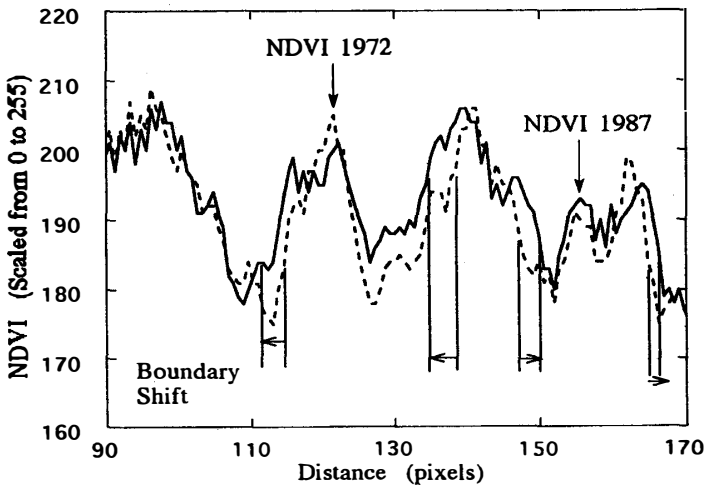

Fig. 4. Profile Showing Vegetation Boundary Shift. These profiles extends over 600 m near the circle A in Fig 2.

$$\mathrm{NDVIs}(i)=\sum_{j=-n}^{n} w(j)\times \mathrm{NDVI}(i+j), \tag{4}$$

where

j	$-n$	$-n+1$	...	-1	0	$+1$	...	$n-1$	n	pixels,
					i					

$w(j)$: linear weight for the $(i+j)$th pixel
for $j = -n$ & n, $-(n-1)$ & $n-1$, ... , -1 & 1, 0,
$w(j)=1/d$, $2/d$, ... , n/d, $(n+1)/d$.
Total of $w(j)$ is 1.

d: $\sum_{j=-n}^{n} (n+1-\sqrt{j^2})$,

n: $2\times n+1$ is the number of pixels used for smoothing,
NDVI $(i+j)$: NDVI of the $(i+j)$th pixel,
NDVIs(i): smoothed NDVI of the i-th pixel.

The first derivative of the smoothed profile was calculated from the smoothed NDVI as follows.

Calculating derivative:

$$\mathrm{NDVIs}'(i)=(\mathrm{NDVIs}(i+1)-\mathrm{NDVIs}(i)), \tag{5}$$

where

NDVIs(i): NDVI of i-th pixel,
NDVIs'(i): the first derivative of i-th pixel.

The second derivative was calculated by repeating operations (4) and (5) (Fig 6). Then vegetation boundary positions, which were defined as the zero position in the second derivative profiles, were visually compared with boundaries of the original NDVI profiles.

This combination of smoothing and derivative analysis was applied for the two NDVI images as follows. A weighting matrix of the linear-weighting running-average smoothing to apply to the NDVI images were defined (Table 1) as follows.

Defining weighting matrix :

When $\sqrt{i^2+j^2}<n+1$

$$D=\sum_{i=-n}^{n}\sum_{j=-n}^{n} (n+1-\sqrt{i^2+j^2}), \tag{6}$$

$$Wij=(n+1-\sqrt{i^2+j^2})/D, \quad (7)$$

other than $\sqrt{i^2+j^2}<n+1$,

$$Wij=0, \quad (8)$$

where

$2n+1$: matrix size,
i: column number $i=n,-n$,
j: line number $j=n,-n$,
Wij: weight for i-th column, j-th line in the weighting matrix. Total of Wij is 1.

The NDVI images were smoothed using the weighting matrix. Then a Laplacian operator (TAKAGI and SHIMODA, 1991, Table 1) was applied to the smoothed NDVI images to compute the second derivative (Fig. 7). The final resultant image (Fig. 8) was created from the two second derivative images according to Table 2.

Table 1. Filtering kernels of a linear-weighting running-average (A) and a laplacian (B).

	A. Linear weight*						B. Laplacian filter			
Column	1st (11th)	2nd (10th)	3rd (9th)	4th (8th)	5th (7th)	6th				
							Column	1st	2nd	3rd
1st (11th)	0	0	0.75	2.72	3.98	4.42	1st line	1	1	1
2nd (10th)	0	1.52	4.42	6.76	8.30	8.85	2nd	1	−8	1
3rd (9th)	0.75	4.42	7.77	10.59	12.55	13.27	3rd	1	1	1
4th (8th)	2.72	6.76	10.59	14.03	16.65	17.69				
5th (7th)	3.98	8.30	12.55	16.65	20.28	22.11				
6th line	4.42	8.85	13.27	17.69	22.11	26.53				
					($\times 10^{-3}$)					

*The upper left quarter of linear-weights are shown. The other three quarters of the matrix are mirror duplicates of this quarter and they are shown in parenthesis.

Table 2. Colors in the Fig. 8.

	Digital numbers in laplacian images		Colors in Fig. 8	Boundaries
	1972	1987		
Case1	≧0	≧0	black	
Case2	<0	≧0	red-orange	advanced
Case3	≧0	<0	blue	receded
Case4	<0	<0	gray	

5. Results and Discussion

Water and rock are very often used as spectrally pseudo-invariant standards in spectral calibration. Although spectral invariability of the standards, *ex* the lake water and the rock outcrop, was not confirmed, the intensities of the two NDVI images agreed very well. This intensity matching were good enough to make visual comparison of the vegetation boundaries in profiles easy.

The profiles clearly showed the location of the peaks and slopes of the NDVI pattern (Fig. 4). Thus comparison of profile patterns seems to be an effective method for boundary shift detection. The 1972 and 1987 profiles suggest expansion of the vegetation over the 15 year period. The 1972 profile is narrower between pixel distances 135 to 150 than the 1987 profile, and the maximum NDVI value appears at the same location (140). Phenological factors may not be the reason for the widening of the peak in Fig. 4. Since the intensities of the two NDVI images were adjusted to each other, the same amplitude at the same locations in the two NDVI images probably shows unchanged vegetation there. Almost equal intensities at the peak (140), the valley (150) and the slope from 90 to 105 showed little change in vegetation. The profile spanned only about 600 meters, then vegetation there would be under a very similar phenological stage. Moreover, since the NDVI increases exponentially against the LAI (ASRAR *et al.*, 1989), the NDVI shows small amount of vegetation and its changes in smaller intensities. These suggest that the vegetation, peaking at 140, would become denser around the peak, then intensities from 125 to 150, for example, in the 1987 profile become greater than these in 1972. If the predicted vegetation migration occurred, numerous larger shifts than those in Fig. 4 would be observed.

The smoothed profiles (Fig. 5) matched well with the original profiles maintaining the major pattern, and boundaries were also clearly identified on

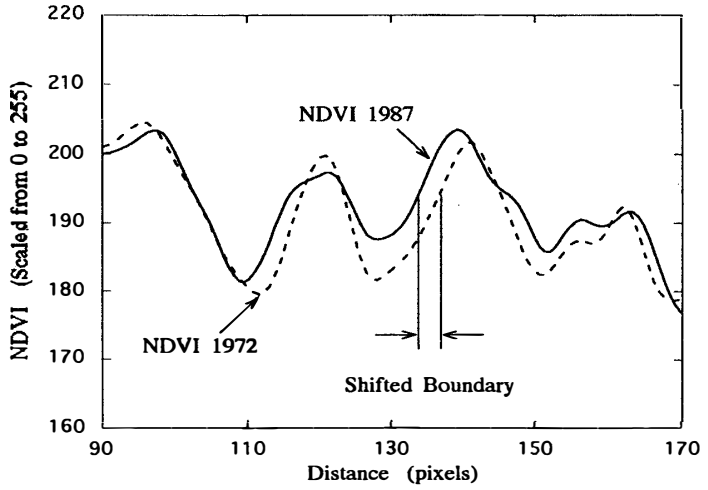

Fig. 5. Smoothed Profile of Fig. 4 Using The Linear-Weighting Running-Average Smoothing.

them. Since derivatives are noise sensitive operations, this smoothed profile made the derivative analysis possible. The zero of the second derivative in the derivative profiles (Fig. 6), which was defined as vegetation boundary, was satisfactorily well appeared in accordance with the slopes in the original NDVI profiles (Fig. 4). This result suggests that application of the second derivative is probably useful for detection and monitoring of vegetation boundary positions. But minor peaks also yielded zero (Fig. 6) and these will disturb accurate change detection. Further study for selecting the best combination of smoothing, a laplacian filter

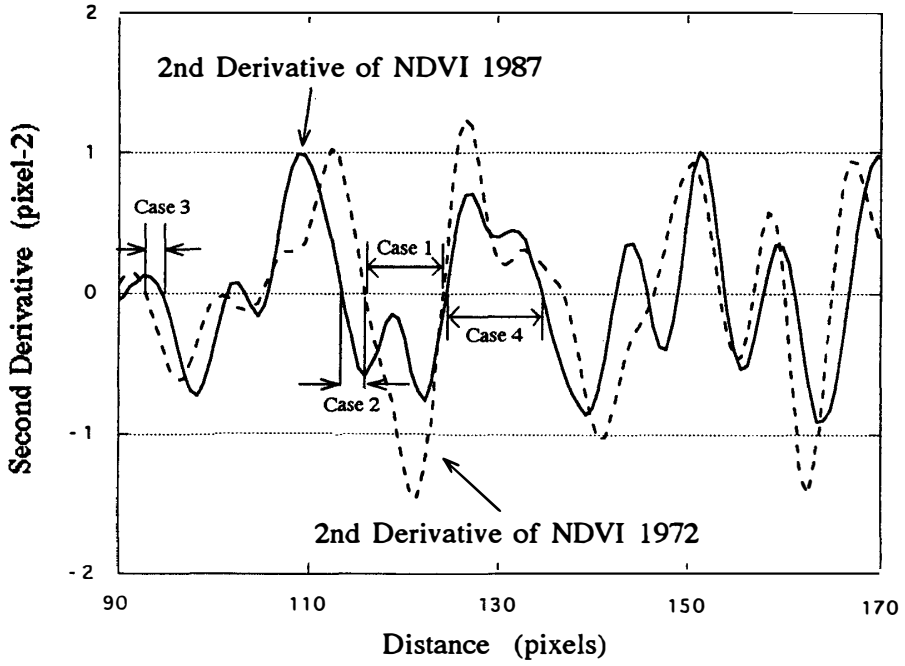

Fig. 6. Second Derivative of Fig. 5. The cases from 1 to 4 are corresponding to the cases in Table 2.

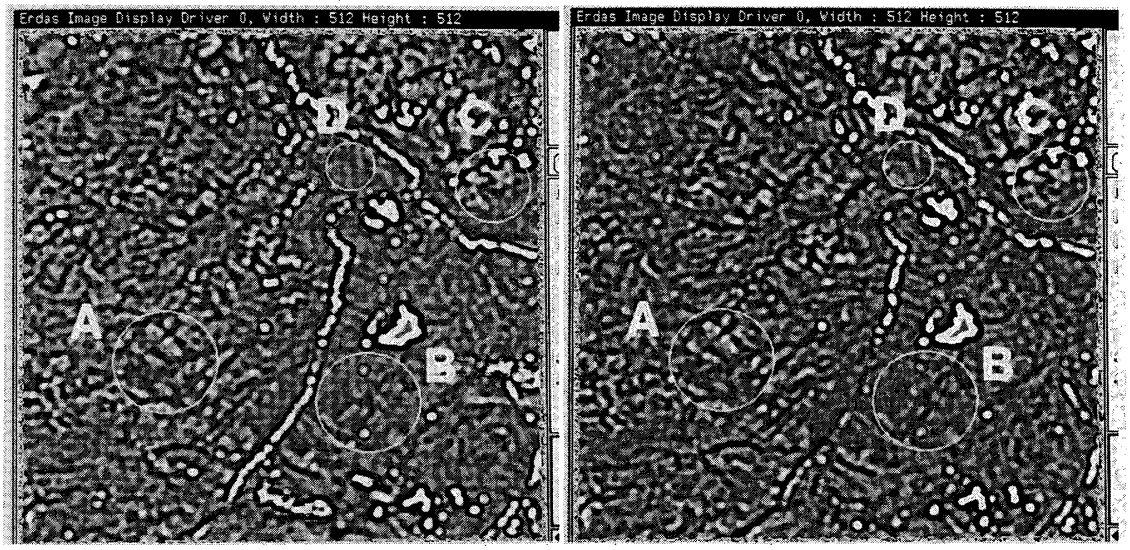

Fig. 7. The Second Derivative Images (results of Laplacian Filtering) of 1972 (left) and 1987 (right) NDVI.

and a removal method of minor changes is necessary to analyze boundary positions more accurately without noise disturbances.

Figure 8 was created from the second derivative images (Fig. 7) according to Table 2. Red-orange and blue shows advancing and receding of the vegetated area respectively. Since clouds and very dark topographic shadows (Fig. 2), which appeared differently in the two images, disturbed boundary analysis and interpretation, those areas are also masked out in black in Fig. 8. Boundary lines in the two derivative images agreed within a few pixels as a whole. However, numerous red-orange and blue patches, which were wider than 3 pixels and probably showed boundary changes, appeared.

Four cloud free areas, which represented typical vegetation types in the study site, were marked in figures (Figs. 2, 8) to make clear the locations to describe tendency of detected changes in different vegetation types. Vegetation types included birch mire forests and treeless tundra in A, birch forests in B, birch-pine forests and treeless tundra in C, and birch-pine forests in D. Fairly big disturbances of vegetation boundaries were observed within circle B, especially in the left side. Since mountain birches were dominant and have been damaged by the moss caterpillar there (NATIONAL BOARD OF SURVEY, 1988), the damage might be the cause of the disturbance. One big disagreement of boundaries was also observed around birch mire (near the center of Circle A), and difference in spectra was identifiable in comparison between the two MSS image color composites. The disagreement might be caused by the different phenological stages of vegetation in the two MSS images. Small changes were observed in or between pine forests and birch forests (Circle C and D).

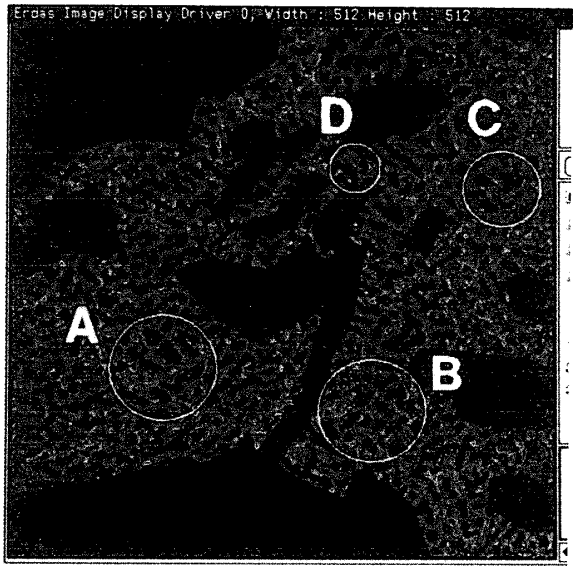

Fig. 8. Recoded Image of The Second Derivative for A Vegetation Boundary Comparison. See Table 2 and Fig. 6 for the meaning of colours. A majority filtering within 3 by 3 pixel-kernel was applied for this result to remove noises and errors. Receding and advancing of boundaries showed that there were many small changes in vegetation or its spectra.

Both advancing and receding of boundaries were detected in vegetated areas, and this would suggest that most of the detected small changes were probably insignificant seasonal spectral changes of vegetation. However, very significant changes can be chosen by identifying clear boundaries using local amplitude of NDVI images (AWAYA and TANAKA, 1993). Since the cause of the changes cannot be revealed by satellite data, a ground check is necessary to confirm vegetation changes and their cause. Such a ground check will make clear how worthy large changes in vegetation boundaries is to examine.

6. Conclusion

The change detection method which was described in this paper showed rather small changes in vegetation boundaries. This would support utilization of satellite data for vegetation shift monitoring, after significant changes are selected well. Once the best combination of smoothing and Laplacian filters are found, the method requires little operator skill and yields steady output. This makes stable data processing possible scene by scene, which is the main advantage of the method.

On the other hand, following are two major weakness of this method.

(1) If boundaries shift greatly, it may be difficult to identify corresponding boundaries in different images, which show past and present vegetation, and more than two images are required.

(2) Since this method does not show vegetation types at border lines, they have to be identified by a different manner.

Though large vegetational migrations have been predicted to accompany global warming, temperature trends show insignificant changes in Fennoscandia. This test case of vegetation boundary monitoring in northern Finland using Landsat MSS showed numerous advancing and receding small boundary changes. These probably suggest that small vegetational changes were quite common in the study site and most of them were seasonal spectral changes. Then it is the main obstacle of this method to separate significant long term changes from seasonal changes by image processing. The analysis method is under development and should be improved a selection of significant changes. Thus no clear evidence of vegetation migration was obserbed.

It may be difficult to detect the initial stages of vegetation change using satellite data only, but results using the change detection system should provide helpful information for ground checking. Vegetation monitoring is very important for understanding the ecological environment, and the status of global vegetation. Satellite remote sensing may be the most useful tool for monitoring vegetation changes in the boreal areas. The monitoring methods, developed in this study can be used for long term monitoring of changes in the vegetation cover.

Acknowledgment

This study was carried out as part of the 'Japanese Experimental Study in the Arctic Area' supported by the Science and Technology Agency of Japan. The authors appreciate their support. This paper is part of the presentation by Dr. AKIYAMA of the National Institute of Agro-Environmental Sciences in the XV Symposium on Polar Biology, which was titled 'Effects of Vegetational and Phenological Changes on Spectral Reflectance in the Arctic Area'.

References

ASRAR, G., MYNENI, R. B. and KANEMASU, E. T. (1989): Estimation of plant-canopy attributes from spectral reflectance measurements. Theory and Applications of Optical Remote Sensing, ed. by G. ASRAR. New York, J. Wiley, 252–296.

AWAYA, Y. and TANAKA, N. (1993): Vegetation change detection with a laplacian filter using Landsat data - A case study in a boreal forest-tundra transition area. International Geoscience and Remote Sensing Symposium (IGARSS'93), Vol II, 743–746.

AWAYA, Y., MILLER, J. R. and FREEMANTLE, J. R. (1992): Background Effects on Reflectance and Derivatives in an Open-Canopy Forest Using Airborne Imaging Spectrometer Data. International Achieves of Photogrammetry and Remote Sensing, XXIX B7, 836–843.

BOER, M, M., KOSTER, E. A. and LUNDBERG, H. (1990): Greenhouse impact in Fennoscandia-Preliminary findings of a European workshop on the effects of climatic change. Ambio, **19**, 2–10.

EMANUEL, W. R., SHUGART, H. H. and STEVENSON, M. P. (1985): Climatic change and the broad-scale distribution of terrestrial ecosystem complexes. Clim. Change, **7**, 29–43.

GATES, D. M. (1990): Climate change and the response of forests. Int. J. Remote Sensing, **11**, 1095–1107.

HÄME, T. (1991): Spectral interpretation of changes in forest using satellite scanner images. Acta For. Fenn., **222**, 111 p.

HEINO, R. (1992): Climate changes in Northern Europe. The Finnish Research Programme on Climate Change, ed. by M. KANNINEN and P. ANTTILA. Helsinki, Govn. Printing Center, 25–26.

KENNEWEG, H., FOSTER, B., RUNKEL, M. and WINTER, R. (1988): Satellitenbilder zur waldschadenserfassung–Wo liegen die probleme? Allg. For.-Jagdzig., **160**, 73–76.

MOONEY, H. A., DRAKE, B. G., LUXMOORE, R. J., OECHEL, W. C. and PITELKA, L. F. (1991): Predicting ecosystem responses to elevated CO_2 concentrations. BioScience, **41–2**, 96–104.

NATIONAL BOARD OF SURVEY, ed. (1988): Atlas of Finland. Climate 131, Biogeography, Nature Conservation. Helsinki, National Board of Survey, 141–143.

OHMURA, S. *et al.* (1991): IPCC Chikyû Ondan-ka Report. Kasumigaseki Chikyû Ondan-ka Mondai Kenkyûkai. Tokyo, Chûô Hôki Shuppan, 115–116.

OVERPECK, J. T., BARTLEIN, P. J., WEBB, T., III (1991): Potential magnitude of future vegetation change in eastern North America: Comparisons with the past. Science, **254**, 692–695.

RESTEC, ed. (1986): Chikyû Kansoku Dêta Riyô Handobukku–Randosatto-hen Kaitei-ban–. Tokyo, RESTEC, Sec. 6, 1.

SHUGART, H. H., LEEMANS, R. and BONAN, G. B., ed. (1992): A Systems Analysis of the Global Boreal Forest. Cambridge, Cambridge Univ. Press, 126–267.

SINGH, T. and WHEATON, E. E. (1991): Boreal forest sensitivity to global warming: Implications for forest management in western interior Canada. For. Chron., **67**, 342–48.

TAKAGI, M. and SHIMODA, H. (1991): Gazô Kaiseki Handobukku (Handbook of Image Analysis). Tokyo, Tokyo Daigaku Shuppankai, 550–553.

(Received April 19, 1993; Revised manuscript received August 24, 1993)